

**DEVELOPMENT OF A MECHANISTIC MODEL FOR PREDICTING CORROSION RATE IN
MULTIPHASE OIL/WATER/GAS FLOWS**

**R. ZHANG, M. GOPAL, AND W. P. JEPSON
NSF, I/UCRC CORROSION IN MULTIPHASE SYSTEMS CENTER
DEPARTMENT OF CHEMICAL ENGINEERING
OHIO UNIVERSITY, ATHENS, OHIO, USA**

ABSTRACT

A mechanistic model has been developed to predict corrosion rates in multiphase (water/oil/CO₂) flow conditions. The model takes into account electrochemistry, reaction kinetics, and, mass transport effects. This paper describes the equations used to determine pH and bulk concentrations of various ions, which are then used to calculate the mass transfer rates to the corrosion surface. The result includes the determination of the mass transfer coefficients of various ionic species and corrosion rates. Details of relations used for determination of mass transfer coefficients for multiphase flows, and rates of electrochemical reaction kinetics are discussed and predicted results are compared with experimental observations. Agreement between model results and experimental data is good.

Introduction

Many oil and gas flow lines commonly encounter carbon dioxide and sea water due to the enhanced oil recovery techniques. Carbon dioxide gas dissolves in water to form a weak carbonic acid that is corrosive to many production equipment materials. The degree of corrosion is enhanced by the multiphase flow of oil/saltwater/gas mixtures under conditions of high wall shear. This corrosive media can cause severe damage to pipelines. The prediction of corrosion in carbon dioxide environments typical of oil and gas production has attracted much attention over many years and extensive research has been done to investigate

Copyright

corrosion mechanisms of carbon steel due to carbon dioxide, but adequate models still do not exist.

Most models are based on experiments carried out in stirred beakers, rotating cylinder electrodes and small diameter pipes. Correction factors applied to these predicted corrosion rates cannot be relied on in other environments and the need for basing models on experimental results from large diameter flow loops is imperative. Study of sweet corrosion in multiphase flow requires the prediction of the effects of oil/water composition, flow regimes, and flow characteristics such as, phase distribution and holdup, at different pressures and temperatures on corrosion rates. Such an approach is described in this paper.

Several models for prediction of corrosion rates have been presented over the years. DeWaard and Milliams (1975) studied the mechanisms of carbon dioxide corrosion of carbon steel under various conditions of pH, temperature, and pressure. They proposed the following mechanism for the corrosion process:

Formation of carbonic acid:



Cathodic reaction:

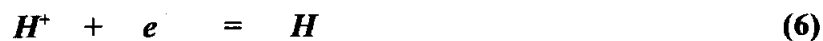


Schmidt (1983) suggested that direct reduction of carbonic acid on the metal surface was also possible. The cathodic reduction still involved hydrogen ion reduction. Wieckowski (1983) suggested that both H_2CO_3 and HCO_3^- reactions took place on the metal surface.

Nesic et al. (1995) proposed a model for carbon dioxide corrosion, based on modeling of individual electrochemical reactions occurring in water-carbon dioxide systems. In their model they began with Equation (1) to describe the formation of carbonic acid in an aqueous solution, and included Equation (2) as the first dissociation step of carbonic acid. They also suggested a second dissociation step for carbonic acid to produce hydrogen ions as follows:



At the surface the reduction of hydrogen ions to hydrogen was given by:



Equation (6) is dominant for $pH < 4$. At an intermediate pH ($4 < pH < 6$), which is the range of primary interest, in addition to the reduction of hydrogen ions, the direct reduction of carbonic acid also becomes important. This reaction is given by:



Dayalan et al. (1995) proposed a mechanistic model for the carbon dioxide corrosion of steel in pipe flow. They suggested that the overall corrosion process can be divided into four steps. The first step is the dissolution of carbon dioxide in the aqueous solution to form the various reactive species which take in the corrosion reaction. The second step is the transportation of these reactants to the metal surface. The third step involves the electrochemical reactions (anodic and cathodic) taking place at the surface. The final step is the transportation of the corrosion products to the bulk of the solution.

The model described in this paper, follows the same principal steps as described by Dayalan et al. (1995). However, a detailed description of pH calculations using ionic activities, and calculation of mass transfer coefficients in single phase and two-phase oil/water flows are given. The number of reaction s corrosion process are also simplified following Herce et al. (1995).

Herce et al. (1995) also showed that the combined effects of CO₂ partial pressure, ionic strength, temperature, and initial bicarbonate ion concentration, i.e. solution chemistry, may be described by a single variable pH. The combined the effects of fluid flow with pH to define hydrogen ion flux which they related to corrosion rate under a variety of conditions.

Empirical Correlations

DeWaard, Lotz, and Dugstad (1995) have shown that in the temperature range of 10-80 C, analysis of the temperature dependence of CO₂ solubility and H₂CO₃ dissociation constants shown that the temperature dependence of the pH can be approximated by:

$$pH_{CO_2} = 3.82 + 0.00384 - 0.5 \log(pCO_2) \quad (8)$$

They further correlated corrosion rate as a function of actual pH, thereby suggesting a linear correlation between corrosion rate and H⁺ concentration at high mass transport rates. However, at lower flow rates, the overall dependence on pH will be less.

Calculation of Bulk Concentrations

It is assumed that the dissolution reaction of iron into the solution does not significantly affect the bulk pH.

Electroneutrality

The composition of ASTM D1152 substitute sea water used in the experiments at the Corrosion Center are shown in Table 1. Seawater primarily contains more than 99.95% Total Dissolved Solids (TDS). These are largely contributed by 11 major constituents including, NaCl, Na₂SO₄, NaHCO₃, NaF, KCl, KBr, MgCl₂, CaCl₂, SrCl₂, and, H₃BO₃. In solution, these compounds dissociate into their constituent ions, and their concentrations along with HCO₃⁻, CO₃²⁻, H⁺, and OH⁻, cannot be varied independently, due to electroneutrality requirements. This may be written as follows:

$$\lambda + [H^+] = [HCO_3^-] + [OH^-] + 2[CO_3^{2-}] \quad (9)$$

where,

$$\lambda = [Na^+] + 2[Mg^{2+}] + 2[Ca^{2+}] + [K^+] + 2[Sr^{2+}] - [Cl^-] - 2[SO_4^{2-}] - [HCO_3^-] - [Br^-] - [(BO)_4^-] - [F^-]$$

The concentration of CO_3^{2-} has been found to not significantly affect the overall corrosion reaction, therefore, the concentration of CO_3^{2-} ions can be neglected in pH calculations. Equation (9) then becomes:

$$\lambda + [H^+] = [HCO_3^-] + [OH^-] \quad (10)$$

The association of all the ionic components of sea salt except H^+ ions, is neglected for the purposes of pH calculations. Their activity coefficients can be taken as $\gamma_i = 1$. Equation (10) can be expressed in terms of activity coefficients as follows:

$$\lambda + \frac{a_{H^+}}{\lambda_{H^+}} = \frac{a_{HCO_3^-}}{\lambda_{HCO_3^-}} + \frac{a_{OH^-}}{\lambda_{OH^-}} \quad (11)$$

Carbon dioxide Ionization

The equilibrium thermodynamic constant for the dissociation of H_2CO_3 by Equation (2) is given by:

$$K_{1,CO_2} = \frac{a_{H^+} \cdot a_{HCO_3^-}}{a_{CO_2}} \quad (12)$$

Carbon Dioxide solubility

It is assumed that the entire CO_2 in solution dissolves to form H_2CO_3 . The dissolution of carbon dioxide in solution is given by Henry's law as follows:

$$a_{CO_2} = f_{CO_2} K_H \quad (13)$$

where,

a_{CO_2}	=	activity of CO_2 in liquid phase
f_{CO_2}	=	fugacity of CO_2 in the gas phase = $y_{CO_2} \phi_{CO_2} P_T$
ϕ_{CO_2}	=	fugacity of CO_2 in the gas phase
y_{CO_2}	=	mole fraction of CO_2 in the gas phase
P_T	=	total pressure of the system
K_H	=	Henry's law constant

The fugacity coefficient of carbon dioxide is nearly 1 for pressures less than 25 bars, which is the range of interest for this study.

Dissociation of water

Concentration of free H^+ and OH^- ions are related by the ionic product of water as:



$$K_w = \frac{a_{H^+} \cdot a_{OH^-}}{a_{H_2O}} \quad (15)$$

Activity of Hydrogen

The activity of water under standard conditions is equal to 1. Also, for dilute aqueous solutions the activity coefficient of water can be taken as unity. Equation (12) can then be written in terms of a_{H^+} , a_{CO_2} , the ionization constants and activity coefficients as:

$$\frac{1}{\gamma_{H^+}} a_{H^+}^2 + \lambda a_{H^+} + \left[-\frac{K_1 CO_2 \cdot a_{CO_2}}{\gamma_{HCO_3^-}} - \frac{K_w}{\gamma_{OH^-}} \right] = 0 \quad (16)$$

Equation (16) can be solved for a_{H^+} , if all the ionization constants can be estimated as functions of temperature and pressure.

Equilibrium Constants

Pitzer (1991) suggested that the chemistry of carbon dioxide is controlled by the following equilibria:



Combining Equations (16) and (17)



He proposed the following fitting parameters for $K_{HCO_3^-}$.

$$pK_{HCO_3^-} = 6320.81 / T - 126.3405 + 19.568 \ln T \quad (21)$$

And for Henry's law:

$$\log(K_H) = 108.3865 + 0.01985076 T - 6919.53 / T - 40.45154 \log(T) + 669365 / T \quad (22)$$

He related the total alkalinity in seawater by taking into account the equilibria:



The dissociation constant of water is given by Wagman et al. (1982) as:

$$\log(K_{H_2O}) = -283.971 + 13323/T - 0.05069842 T + 102.24447 \log(T) - 1119669 / T^2 \quad (25)$$

The dissociation constant $K_{B(OH)_4}$ suggested by Pitzer (1991) is:

$$\ln(K_{B(OH)_4}) = (-8966.9 - 2890.51 S^{1/2} - 77.942 S + 1.726 S^{3/2} - 0.0993 S^2) / T + (148.0248 + 137.194 S^{1/2} + 1.62247 S) + (-24.4344 - 25.085 S^{1/2} - 0.247 S) \ln(T) + 0.053105 S^{1/2} T \quad (26)$$

where, $S = \text{Salinity} = 1.80655 \text{ Cl}\%$
 $\text{Cl}\% = \text{chlorinity} = S_T / 1.81638$
 $S_T = \text{Total salt content g/kg seawater}$

Activity Coefficients

The Debye Huckel equation was modified by Davies for the mean activity coefficient as:

$$\log \gamma_{\pm} = -A z_+ |z_-| \left(\frac{\mu^{1/2}}{1 + \mu^{1/2}} - 0.3\mu \right) \quad (27)$$

where $\mu = \text{ionic strength on the molality scale}$
 $z = \text{ionic charge}$
 $A = 1.82e6(\epsilon T)^{-3/2}$
 $\epsilon = \text{dielectric constant}$
 $T = \text{Temperature, K}$

Ionic strength is determined as:

$$\mu = \frac{1}{2} \sum_j z_j^2 m_j \quad (28)$$

where, $m_j = \text{molality of ion } j \text{ with charge } z$

In using the Davies equation in a solution containing several electrolytes (as is the case here) all the ions in the solution contribute to μ . However, z in Equation (27) refers to the ionic charge of the particular electrolyte for which γ_{\pm} is being calculated. Moreover, the Davies Equation for $\log \gamma_{\pm}$ is obtained by replacement of $z_+ |z_-|$ in Equation (26) by z^2 .

Dielectric Constant for Water

Pitzer has suggested the following correlation for evaluating the dielectric constant for water. This is dependent on pressure and temperature:

$$\epsilon = \epsilon_{1000} + C \ln[(B+P)/(B+100)] \quad (29)$$

where, P = Total pressure, bars

The temperature dependence is given by:

$$\epsilon_{1000} = U_1 \exp(U_2 T + U_3 T^2) \quad (30)$$

$$C = U_4 + U_5 / (U_6 + T) \quad (31)$$

$$B = U_7 + U_8 / T + U_9 / T \quad (32)$$

where, T = temperature, K

Calculation Procedure

Initially, the activity coefficients of H^+ , HCO_3^- , and OH^- ion are assumed equal to unity and the ionic concentrations calculated. These ionic concentrations are then used to calculate the ionic strength of the solution which in turn is used to calculate the activity coefficients for the ions. Equation (16) is then solved iteratively for the activity of hydrogen ion (and hence the pH) for various temperatures and pressures.

Mass Transfer Coefficients

Mass transfer plays an important role in the corrosion process. Due to electrochemical reactions taking place on the metal surface, the concentrations of various species at the metal surface are different from those in the bulk. As a result of this concentration gradient in the fluid, there is a movement of the species from the bulk to the pipe wall and vice-versa. In order to calculate the mass transfer flux of the species it is necessary to compute the mass transfer coefficients of the species. The empirical Chilton-Colburn equation for turbulent transfer [20] predicts that :

$$K_{mt} = \frac{f Re D Sc^{1/3}}{8 d} \quad (33)$$

where, K_{mt} = mass transfer coefficient of the species
 Re = Reynold's number of the fluid = $\rho v d / \mu$
 Sc = Schmidt number = $v / D = \mu / (\rho D)$
 D = diffusivity of the species in the fluid
 f = moody friction factor
 d = diameter of the pipe

The semi-empirical Vieth et al. Expression () for fully developed turbulent mass transfer predicts that:

$$K_{mt} = \frac{4.586 \left(\frac{V_{max}}{V_{avg}} \right) f Re D (Sc)^{1/3}}{8d} \quad (34)$$

where,

- K_{mt} = mass transfer coefficient of the species
- Re = Reynold's number of the fluid $= \rho v d / \mu$
- Sc = Schmidt number $= \nu / D = \mu / (\rho D)$
- D = diffusivity of the species in the fluid
- f = moody friction factor
- d = diameter of the pipe
- V_{max} = maximum velocity in the pipe
- V_{avg} = average velocity in the pipe

The semianalytical Deissler Expressions for turbulent transfer predicts that :

$$K_{mt} = \frac{0.0789 \left(\frac{f}{4} \right)^{1/2} Re D Sc^{1/4}}{d} \quad (35)$$

Another Deissler Expression for turbulent transfer predicts that :

$$K_{mt} = \frac{0.115 \left(\frac{f}{8} \right)^{0.5} Re D Sc^{0.25}}{d} \quad (36)$$

The Chilton-Colburn equation can be generalized for the rough pipes by using an appropriate friction factor. The Moody friction factor can be calculated using the correlation :

$$f^{-1/2} = -1.8 \log_{10} \left[\frac{6.9}{Re} + \frac{(e/d)^{1.11}}{3.7} \right] \quad (37)$$

where,

- e = roughness of the pipe
- d = diameter of the pipe
- Re = Reynold's number

The diffusion coefficients of the ions is calculated using the following correlation:

$$D_i = \frac{\lambda_i R T}{F^2 Z_i} \quad (38)$$

where,	D_i	=	Diffusion coefficient
	λ	=	ionic conductivity
	R	=	universal gas constant
	T	=	temperature (K)
	Z	=	charge of the ion

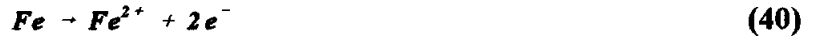
Rates of Electrochemical Reactions:

After the various reactive reach the metal surface, various electron transfer reactions take place between the metal surface and the species. The model assumes that the following reactions take place at the metal surface,

Cathodic reaction:



Anodic reaction:



The current densities due the above electrochemical reactions are given by the Butler-Volmer equation, and can be written as:

$$i_{Fe^{2+}} = 2F K_{e,Fe^{2+}} [Fe^{2+}]_s \exp\left[\frac{2(1-\alpha)F(E_{corr} - E_{Fe^{2+}})}{RT}\right] \quad (41)$$

$$i_{H^+} = 2F K_{e,H^+} [H^+]_s \exp\left[\frac{-2\alpha F(E_{corr} - E_{H^+})}{RT}\right] \quad (42)$$

K_{e,H^+} And $K_{e,Fe^{2+}}$ Are the rate constants for the cathodic and anodic reactions, respectively. The values of the rate constants can be obtained from the literature.

The equilibrium potentials E_{H^+} And $E_{Fe^{2+}}$ are given by the Nernst equations

$$E_{H^+} = E_{H^+}^0 + \frac{RT}{nF} \ln \frac{[H^+]_s}{[H_2]} \quad (43)$$

$$E_{Fe^{2+}} = E_{Fe^{2+}}^0 + \frac{RT}{nF} \ln [Fe^{2+}]_s \quad (44)$$

where, $E_{H^+}^0$ And $E_{Fe^{2+}}^0$ are the standard potentials for the cathodic and anodic reactions.

The sum of the currents due to the cathodic reactions should be equal to the sum of the currents due to the anodic reactions, which in turn is equal to the corrosion current.

$$i_{H^+} = i_{Fe^{2+}} = i_{corr} \quad (45)$$

For iron

$$\text{corrosion rate (mm/year)} = i_{corr} \text{ (amp/cm}^2\text{)} \times (1.16 \times 10^4)$$

Under steady state conditions it is assumed that the sum of the mass transfer rates of the reactants are equal to the sum of the electrochemical reaction rates. Hence we can write,

$$2FK_{m,Fe^{2+}}([Fe^{2+}]_s - [Fe^{2+}]_b) = i_{Fe^{2+}} \quad (46)$$

$$2FK_{m,H^+}([H^+]_b - [H^+]_s) = i_{H^+} \quad (47)$$

the subscripts s and b indict the surface and bulk, respectively.

Results and Discussion

Extensive results on corrosion and multiphase flow have been generated at the NSF, I/UCRC Corrosion in Multiphase Systems Center at Ohio University (Zhou and Jepson, 1993, Jepson and Menezes, 1994, Bhongale et al., 1996). Corrosion and flow data have been measured in 10 cm diameter pipes, at temperatures ranging from 30 C to 90 C, carbon dioxide partial pressures from 0.13 MPa (5 psig) to 0.79 MPa (100 psig), using oil/saltwater mixtures in the liquid phase and carbon dioxide as the gas. Oil/saltwater mixtures ranging from 20% to 100% saltwater have been investigated. ASTM substitute seawater has been for the aqueous phase. Oils of viscosities 2 and 100 cP have been studied. The results from the model are compared with the experimental data obtained using the 2 cP oil. The experimental setup and measurement procedures have discussed extensively in previous papers (eg Bhongale et al., 1996).

pH Results

Figure 1 shows the predicted values of pH for various conditions of pressure and temperature for saltwater solutions. Predicted values of pH for some of these conditions are compared with experimental results in Figure 2.

It is seen from Figure 1 that the pH of the solution decreases from about 5 to 4.2 with increase in carbon dioxide partial pressure from 0.13 MPa to 0.79 MPa. At each pressure, the pH of the solution

increases with increasing temperature. For example, at 0.13 MPa, the pH increases from 5 to about 5.4 as the temperature is increased from 40 C to 90 C. Both results are expected since the dissolution of carbon dioxide in the aqueous solutions increases with pressure, but decreases with temperature.

Comparison with experimental data shows reasonable agreement at all temperatures and pressures. Further, it has been noticed that the pH does not change appreciably when oil is added to solution. Hence the results from the pH calculations are used for oil/water flows as well.

Mass Transfer Coefficients

Selman and Tobias () have summarized several correlations for mass transfer coefficient calculations in turbulent single phase pipe flow. Most of these are applicable over a wide range of Reynolds and Schmidt numbers. However, it is found that the calculated mass transfer coefficients, while in the same order of magnitude, vary widely. Results using three different correlations, the Chilton and Colburn (1957), Deissler et al. (1955), and Vieth et al. (1963), are shown in Tables 2, 3, and 4. The resulting corrosion rate predicted from the model is compared with experimental results at 40 C, and are shown in Figures 3, 4, and 5.

It is seen from Tables 2, 3, and 4, that the mass transfer coefficients in all cases increase with velocity as is expected. However, the actual values are very different. At a velocity of 1.0 m/s, for a pressure of 0.136 MPa, the mass transfer coefficient for Hydrogen ion is $1.6e-4$ m/s using the Chilton Colburn expression, $2.7e-4$ using the Deissler expression, and $8.83e-4$ using the expression from Vieth et al. The corresponding corrosion rates are seen to be 0.35, 0.58, and, 1.91 mm/yr respectively. Comparison with the experimental corrosion rates in Figures 3,4 and 5 shows that it is only the Vieth expression that results in predicted corrosion rates being reasonable.

Simulations of flow in pipes and in the vicinity of disturbances (Gopal and Jepson, 1995) have shown that the corrosion rate is directly proportional to the turbulent kinetic energy of flow. Nesic and Potlethwaithe (1991) have also found similar results and have expressed the opinion that it is the turbulence characteristics, rather than wall shear stress, calculated from average velocity, that influences the corrosion process. Hence, it is felt that a mass transfer correlation that includes the effect of turbulence explicitly will yield a better estimate of the mass transfer coefficient compared to other types of correlations. Such a correlation is being developed at the Corrosion Center. Among the correlations used in this study, the Vieth et al. expression includes a provision for including the turbulence effects through the ratio of V_{max} / V_{avg} . Hence, this gives a better result in this case.

It is seen that the corrosion rates in all cases increase proportionately to the calculated mass transfer coefficient. For example from Table 2, at a pressure of 0.45 MPa, as the velocity is increased from 0.18 m/s to 1.0 m/s, the mass transfer coefficient for H^+ ion increases from $2.1e-4$ to $8.8e-4$, an increase of about 4 times. The predicted corrosion rate increases proportionately from 0.92 to 3.87. The results at all the other velocities are similar. Hence, in the velocity range studied so far, the corrosion rate is mass transfer controlled.

Oil/Saltwater Flow

No model exists at the present time, for the calculation of mass transfer coefficients in oil/water flows. The

correct expression for the Reynolds and Schmidt numbers to be used in correlations is unknown. Extensive experiments at the Corrosion Center in oil/water flows have shown that several flow regimes can exist in oil/water flows. The results confirm earlier work by Oglesby et al. (1978). At all velocities, for oil percentages up to 60% oil in the liquid, there is a water layer present at the bottom of the pipe in horizontal flow. This layer can flow at an *in situ* velocity which is greater than the oil velocity. A model to predict oil/water flow characteristics has been developed and presented elsewhere (Vedapuri and Jepson, 1997).

Two different mass transfer coefficients were defined for oil/water flows. Both involved approximations with respect to the water velocity, and the density and viscosity to be used in the Reynolds and Schmidt number definitions.

In both methods, the water velocity was estimated as follows; From fluid flow results at the Corrosion Center, the variation of the water holdup with height along the vertical diameter was determined. The height of the water layer was approximated as the h/D at which *in situ* water holdup was 75%. Previous work at the Corrosion Center (Neogi et al., 1994) using such approximations, have yielded good results for three phase oil/water/gas stratified flows. Knowing the water film height, the area occupied by the water layer was used to calculate the water velocity as follows:

$$V_{sw} \cdot A_p = V_w \cdot A_w \quad (48)$$

where,

V_{sw}	=	superficial water velocity = q_w / A_p
A_p	=	cross sectional area of pipe
A_w	=	area occupied by the water layer
V_w	=	water velocity

In the first method, mixture density and mixture viscosity (averaged on a volumetric basis) were used in the definition of Reynolds and Schmidt numbers, while in the second method, only the saltwater density and viscosity were used. In both methods, the pipe diameter was used in the definitions for both dimensionless numbers.

20% oil

Tables 5 and 6 show the results of the mass transfer coefficients defined in the two different ways for 20% oil. From Table 5 and 6, it is seen that the mass transfer coefficient for H^+ ion at a velocity of 1.0 m/s at a pressure of 0.27 MPa, is $1.4e-3$ and $1.76e-3$ m/s respectively. The corresponding predicted corrosion rates are 6.09 and 7.73 mm/yr.

The results from Tables 5 and 6 are plotted in Figures 6 and 7 respectively. It is seen that the variation in corrosion rates are proportional to the difference in physical properties calculated in the two methods. Agreement between experiment and model is reasonable in both cases. For example, as the velocity is increased from 0.56 m/s to 1.0 m/s at a pressure of 0.27 MPa, the corrosion rate predicted from the first method increases from 2.48 mm/yr to 6.09 mm/yr, while the corresponding rates from the second method are 3.11 and 7.73 m/s. The experimental corrosion rate for the same velocities are 4.9 and 5.4 mm/yr.

It is seen that the model overpredicts corrosion rates at the higher pressures. For example, at a pressure of 0.79 MPa, as the velocity is increased from 0.56 to 1.0 m/s, the corrosion rate from the first method

increases from 7.21 mm/yr to 17.68 mm/yr, while the corresponding rates from the second method are 9.02 and 22.46 m/s. The experimental rates are 10.75 and 11.6 mm/yr respectively. This overprediction is due to the effect of corrosion product layers at the higher pressures. This effect is not included in the current model.

60% oil

Tables 7 and 8 describe the variation of mass transfer coefficients for Fe^{2+} and H^+ ions calculated by the two methods, along with the predicted and experimental corrosion rates for 60% oil/saltwater flows. The comparison of model results with experimental data is shown in Figures 8 and 9.

Comparison of the mass transfer coefficient values using the two methods from Table 7 and 8 reveal substantial differences in values. For example, the mass transfer coefficient for H^+ ion, at a velocity of 1.0 m/s from the first method is 7.1×10^{-4} m/s, while using the second method, this increases to 1.26×10^{-3} . The results for all the other velocities at other pressures are similar. The comparison with experimental corrosion rates reveals that the use of actual saltwater properties results in much better agreement with experimental values. For example, at a carbon dioxide pressure of 0.79 MPa, increasing the velocity from 0.28 m/s to 1 m/s, increases the corrosion rate from 10.8 mm/yr to 15.75 mm/yr. The corresponding rates predicted are 10.07 and 16.04 mm/yr.

The agreement between experimental and model values for 60% oil using saltwater properties can be expected, since the water velocity is seen to be controlling in this case. Hence, using the saltwater alone for determining the mass transfer coefficient gives a better estimate of the mass transfer coefficient. In the case of 20% oil, with a 2 cP oil, the variation in physical properties are not significant for the two methods to give substantially different values. However, it is expected that as the oil and water properties diverge, the second method, that using the properties of saltwater alone, with the *in situ* water velocity, in the definition of the dimensionless numbers, will give the more accurate results.

Conclusions

A mechanistic model is presented for the prediction of sweet corrosion rate in two phase oil/saltwater flows. The model incorporates the chemistry of the salt, thermodynamics of carbon dioxide dissolution and dissociation, two phase mass transfer, and, electrochemical kinetics on the metal surface. Good agreement with experimental results is seen.

The calculation of pH includes the activity coefficients of the Hydrogen ion, and this related to the concentration of other neutral ions in the solution. Agreement between the experimentally measured pH values and the model predictions are good.

Mass transfer coefficient predictions in turbulent pipe flow are compared using three different correlations and it is shown that the effect of turbulence on the mass transfer needs to be included in any correlation.

Using the pH calculated for saltwater solutions, and a selected correlation, mass transfer coefficients are calculated for two phase oil salt water flows using a new method. The *in situ* water velocity is used, along with the pipe diameter and saltwater density and viscosity for the calculation of mass transfer coefficients.

It is shown that this definition for two phase oil/saltwater flows results in very good agreement of predicted corrosion rate with experimental data.

For the range of velocities studied, the corrosion rate is mass transfer controlled for two phase oil/water flows.

References

- De Waard, C., and Milliams, D. E., (1975) "Carbonic Acid Corrosion of Carbon Steel", *Corrosion*, Vol. 31, No. 5, pp. 177.
- Schmitt, G., (1983) "Fundamental Aspects of CO₂ Corrosion", *CORROSION/83*, paper no. 43.
- Nesic, S., Postlethwaite, J., and Olsen, S., (1995) "An electrochemical model for prediction of CO₂ Corrosion", *CORROSION/95*, 131/1-131/26.
- Dayalan, E., Vani G., Shadley, J. R., and Shirazi, S. A., Rybicki, E. F., (1995) "Modeling CO₂ Corrosion of Carbon Steel in Pipe Flow", *CORROSION/95*, 118/1-118/24.
- Herce, J. A., Wright, E. J., Efir, K. D., Boros, J. A., Hailey, T. G., (1995) "Effects of Solution Chemistry and Flow on the Corrosion of Carbon Steel in Sweet Production", *CORROSION/95*, paper 111.
- Pitzer, Kenneth S., Editor, "Activity Coefficients in Electrolyte Solutions", 1991, CRC Press.
- J. Robert Selman and Charles W. Tobias, "Mass- Transfer Measurements by the Limiting-Current Technique". *Adv. Chem. Engg.*, Vol. 11, No. 3, pp. 271, (1978).
- Chilton, C.H. , and Colburn, A. P., *Ind. Eng. Chem.* 26, 1183 (1934)
- Vieth. W. R., Porter. J.H., and Sherwood. T.K., *Ind. Eng. Chem. Fundam.* 2.1 (1963).
- Deissler. R. G., N.A.C.A. Report 1210, p 69 (1995).

Table 1 Composition of ASTM grade D1141-52 Sea Salt

Substitute Ocean Water	
Component salt	Composition
NaCl	58.49
MgCl ₂ .6H ₂ O	26.46
Na ₂ SO ₄	9.75
CaCl ₂	2.7
KCl	1.645
NaHCO ₃	0.477
KBr	0.238
H ₃ BO ₃	0.071
SrCl ₂ .6H ₂ O	0.095
NaF	0.007

P (MPa)	U (m/s)	KmtFe (m/s)	KmtH (m/s)	[H⁺] (mol/m³)	CR(pred.) (mm/yr)	CR(exp.) (mm/yr)
0.136	1.0	1.6062E-04	8.8382E-04	9.652E-03	1.91	0.88
	1.3	2.0340E-04	1.1192E-03		2.42	1.23
	1.8	2.7357E-04	1.5053E-03		3.25	1.75
0.27	0.18	3.8214E-05	2.1027E-04	1.957E-02	0.92	2.9
	0.28	5.4289E-05	2.9873E-04		1.31	3.0
	1.0	1.6062E-04	8.8382E-04		3.87	4.25
0.45	0.18	3.8214E-05	2.1027E-04	3.267E-02	1.54	3.4
	0.28	5.4289E-05	2.9873E-04		2.18	5.6
	1.0	1.6062E-04	8.8382E-04		6.46	8.6
0.79	0.18	3.8214E-05	2.1027E-04	5.682E-02	2.67	5.6
	1.0	1.6062E-04	8.8382E-04		11.24	11.4

Table 2 : Using Vieth et al. Expression for fully developed turbulent mass transfer to predict corrosion rates for brine

P (MPa)	U (m/s)	KmtFe (m/s)	KmtH (m/s)	[H⁺] (mol/m³)	CR(pred.) (mm/yr)	CR(exp.) (mm/yr)
0.136	1.0	2.9420E-05	1.6189E-04	9.652E-03	0.35	0.88
	1.3	3.7389E-05	2.0574E-04		0.44	1.23
	1.8	5.0585E-05	2.7835E-04		0.60	1.75
0.27	1.0	2.9420E-05	1.6189E-04	1.957E-02	0.71	4.25
0.45	1.0	2.9420E-05	1.6189E-04	3.267E-02	1.18	8.6
0.79	1.0	2.9420E-05	1.6189E-04	5.682E-02	2.06	11.4

Table 3 : Using Chilton and Colburn Expression for fully developed turbulent mass transfer to predict corrosion rates for brine

P (MPa)	U (m/s)	KmtFe (m/s)	KmtH (m/s)	[H ⁺] (mol/m ³)	CR(pred.) (mm/yr)	CR(exp.) (mm/yr)
0.136	1.0	3.9661E-05	2.7009E-04	9.652E-03	0.58	0.88
	1.3	5.0979E-05	3.4716E-04		0.75	1.23
	1.8	6.9774E-05	4.7515E-04		1.03	1.75
0.27	1.0	3.9661E-05	2.7009E-04	1.957E-02	1.18	4.25
0.45	1.0	3.9661E-05	2.7009E-04	3.267E-02	1.98	8.6
0.79	1.0	3.9661E-05	2.7009E-04	5.682E-02	3.44	11.4

Table 4 : Using Deissler Expression in for fully developed turbulent mass transfer to predict corrosion rates for brine

P (MPa)	Total Mixture Velocity (m/s)	KmtFe (m/s)	KmtH (m/s)	[H ⁺] (mol/m ³)	CR(pred.) (mm/yr)	CR(exp.) (mm/yr)
0.27	0.28	7.1249E-05	3.9205E-04	1.957E-02	1.72	4
	0.56	1.0298E-04	5.6666E-04		2.48	4.9
	1.0	2.5270E-04	1.3905E-03		6.09	5.4
0.45	0.28	7.1249E-05	3.9205E-04	3.267E-02	2.87	6.25
	0.56	1.0298E-04	5.6666E-04		4.14	7.4
	1.0	2.5270E-04	1.3905E-03		10.16	7.9
0.79	0.28	7.1249E-05	3.9205E-04	5.682E-02	4.99	9.2
	0.56	1.0298E-04	5.6666E-04		7.21	10.75
	1.0	2.5270E-04	1.3905E-03		17.68	11.6

Table 5 : Using Vieth et al. Expression for fully developed turbulent mass transfer to predict corrosion rates for 20%LVT-80%Saltwater (75% insitu water, $Re \sim D_{pipe}$, mixture properties)

P (MPa)	Total Mixture Velocity (m/s)	KmtFe (m/s)	KmtH (m/s)	[H⁺] (mol/m³)	CR(pred.) (mm/yr)	CR(exp.) (mm/yr)
0.27	0.28	8.7970E-05	4.8406E-04	1.957E-02	2.12	4
	0.56	1.2892E-04	7.0941E-04		3.11	4.9
	1.0	3.2116E-04	1.7672E-03		7.73	5.4
0.45	0.28	8.7970E-05	4.8406E-04	3.267E-02	3.54	6.25
	0.56	1.2892E-04	7.0941E-04		5.19	7.4
	1.0	3.2116E-04	1.7672E-03		12.91	7.9
0.79	0.28	8.7970E-05	4.8406E-04	5.682E-02	6.16	9.2
	0.56	1.2892E-04	7.0941E-04		9.02	10.75
	1.0	3.2116E-04	1.7672E-03		22.46	11.6

Table 6 : Using Vieth et al. Expression for fully developed turbulent mass transfer to predict corrosion rates for 20%LVT-80%Saltwater (75% insitu water, $Re \sim D_{pipe}$, saltwater properties)

P (MPa)	Total Mixture Velocity (m/s)	KmtFe (m/s)	KmtH (m/s)	[H⁺] (mol/m³)	CR(pred.) (mm/yr)	CR(exp.) (mm/yr)
0.27	0.28	8.3699E-05	4.6056E-04	1.957E-02	2.02	4.3
	0.56	7.6510E-05	4.2100E-04		1.84	5.4
	1.0	1.2904E-04	7.1006E-04		3.11	5.75
0.45	0.28	8.3699E-05	4.6056E-04	3.267E-02	3.37	6.4
	0.56	7.6510E-05	4.2100E-04		3.08	7.9
	1.0	1.2904E-04	7.1006E-04		5.19	8.4
0.79	0.28	8.3699E-05	4.6056E-04	5.682E-02	5.86	10.8
	0.56	7.6510E-05	4.2100E-04		5.35	14.3
	1.0	1.2904E-04	7.1006E-04		9.03	15.75

Table 7: Using Vieth et al. Expression for fully developed turbulent mass transfer to predict corrosion rates for 60%LVT-40%Saltwater (75% insitu water, $Re \sim D_{pipe}$, mixture properties)

P (MPa)	Total Mixture Velocity (m/s)	KmtFe (m/s)	KmtH (m/s)	[H⁺] (mol/m³)	CR(pred.) (mm/yr)	CR(exp.) (mm/yr)
0.27	0.28	1.4397E-04	7.9222E-04	1.957E-02	3.47	4.3
	0.56	1.3102E-04	7.2096E-04		3.16	5.4
	1.0	2.2929E-04	1.2617E-03		5.52	5.75
0.45	0.28	1.4397E-04	7.9222E-04	3.267E-02	5.79	6.4
	0.56	1.3102E-04	7.2096E-04		5.27	7.9
	1.0	2.2929E-04	1.2617E-03		9.22	8.4
0.79	0.28	1.4397E-04	7.9222E-04	5.682E-02	10.07	10.8
	0.56	1.3102E-04	7.2096E-04		9.17	14.3
	1.0	2.2929E-04	1.2617E-03		16.04	15.75

Table 8 : Using Vieth et al. Expression for fully developed turbulent mass transfer to predict corrosion rates for 60%LVT-40%Saltwater (75% insitu water, $Re \sim D_{pipe}$, saltwater properties)

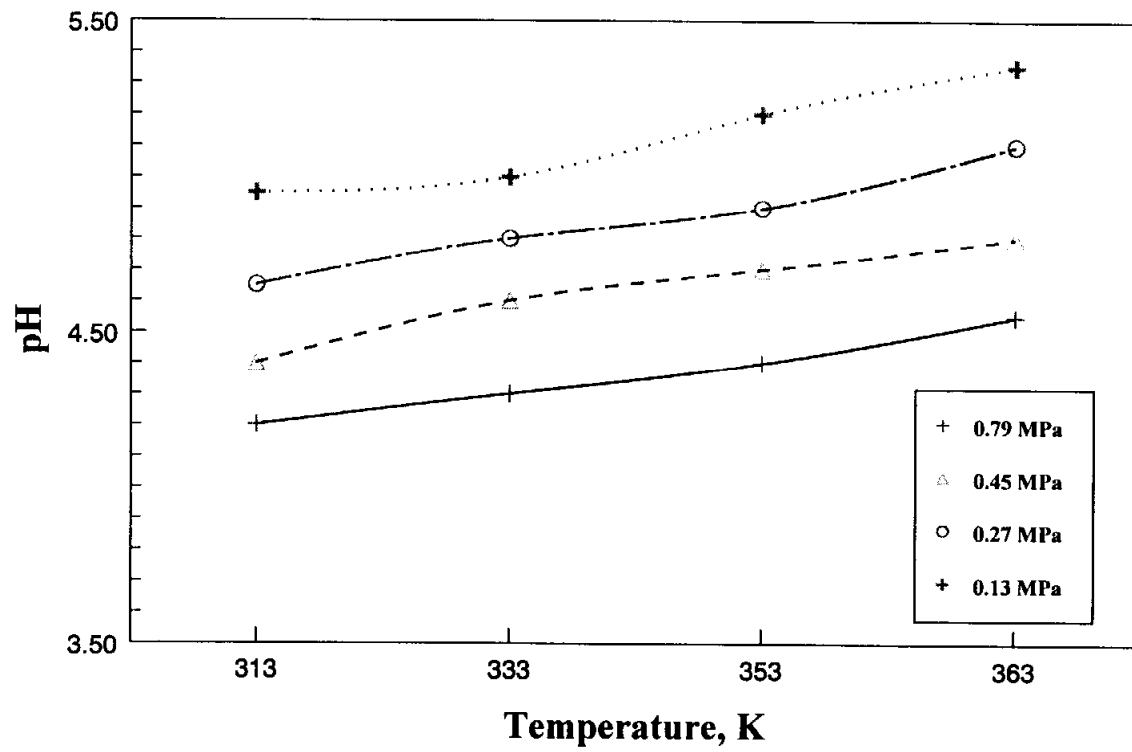


Figure 1: Predicted pH vs Temperature and Pressure

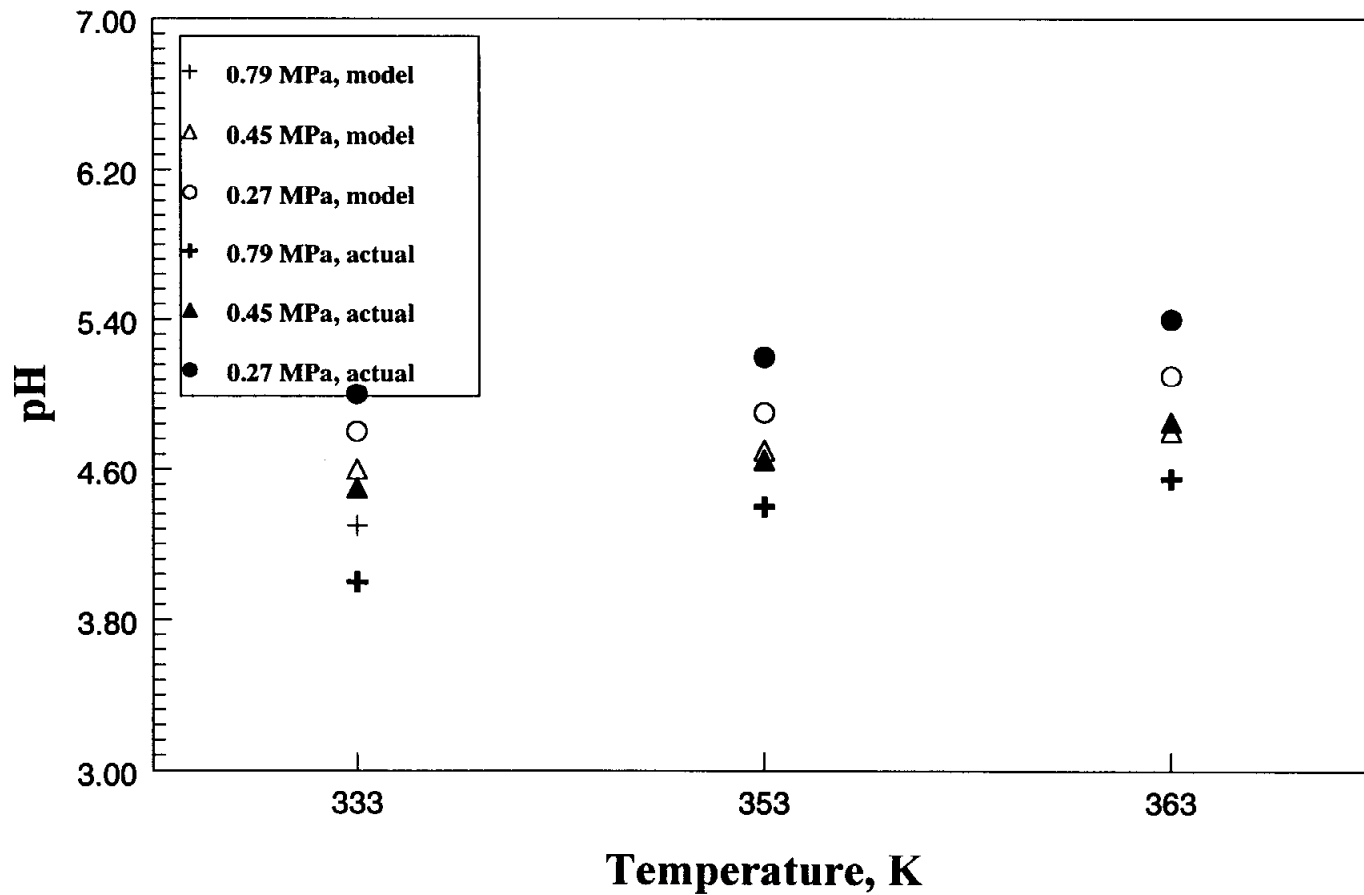


Figure 2: Comparison of Experimental and Model pH values

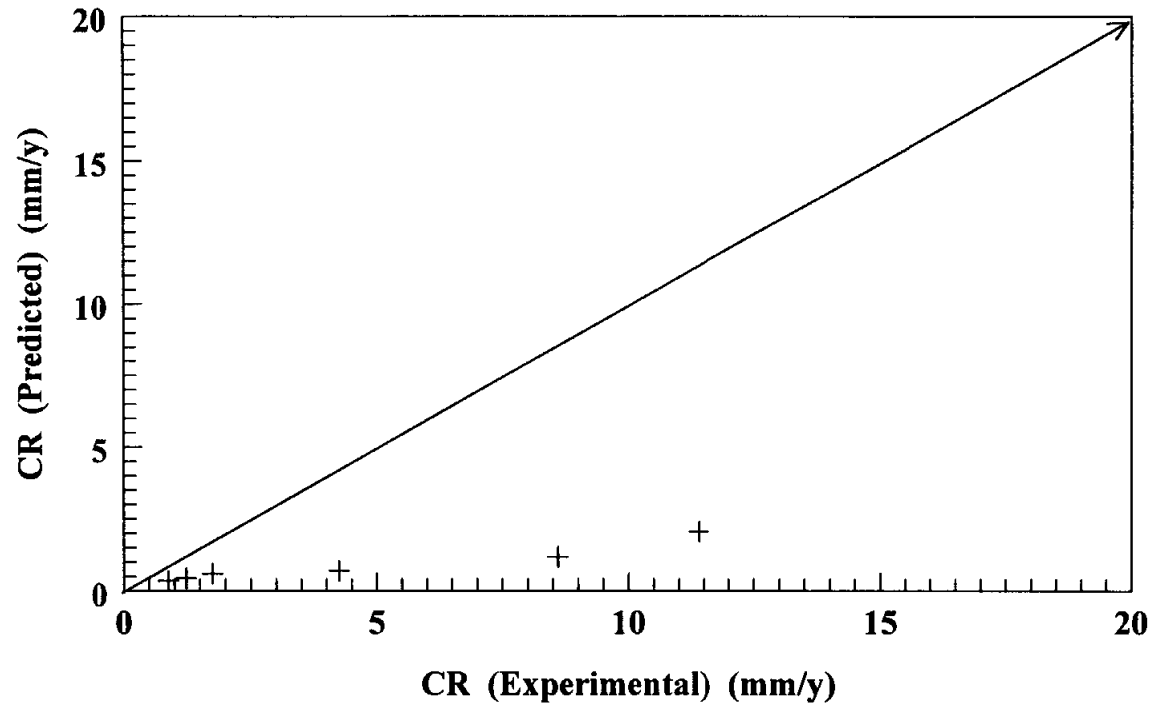


Fig 3: Predicted vs Experimental Corrosion Rates by Using Chilton and Colburn Expression for Mass Transfer

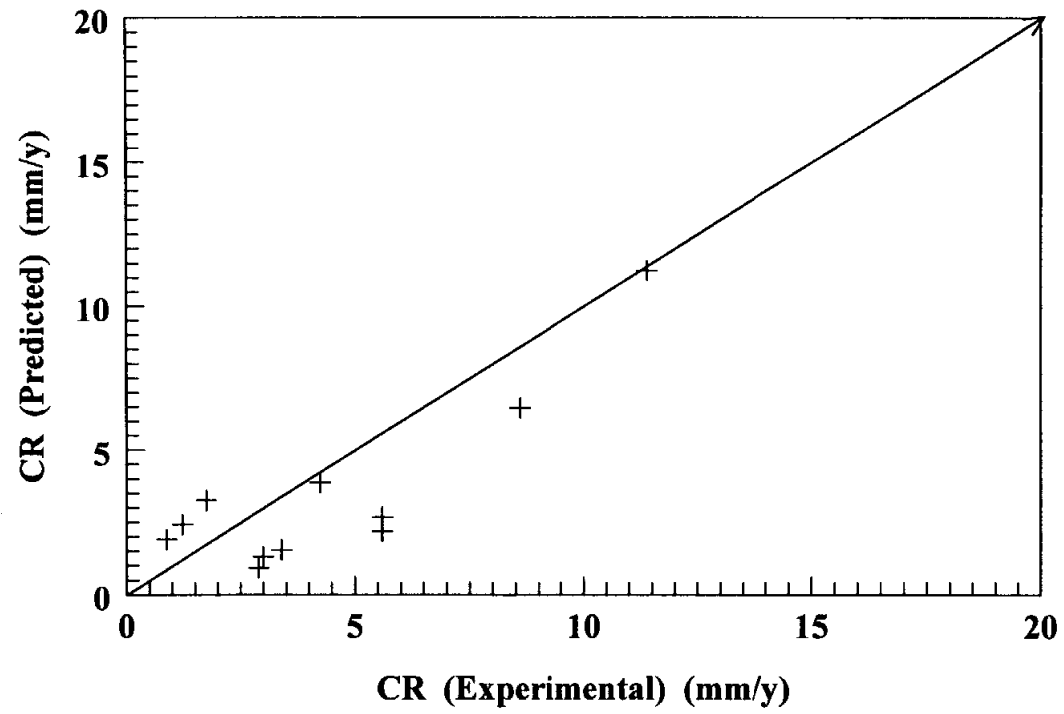


Figure 4: Predicted vs Experimental Corrosion Rates by Using Vieth et al. Expression for Mass Transfer

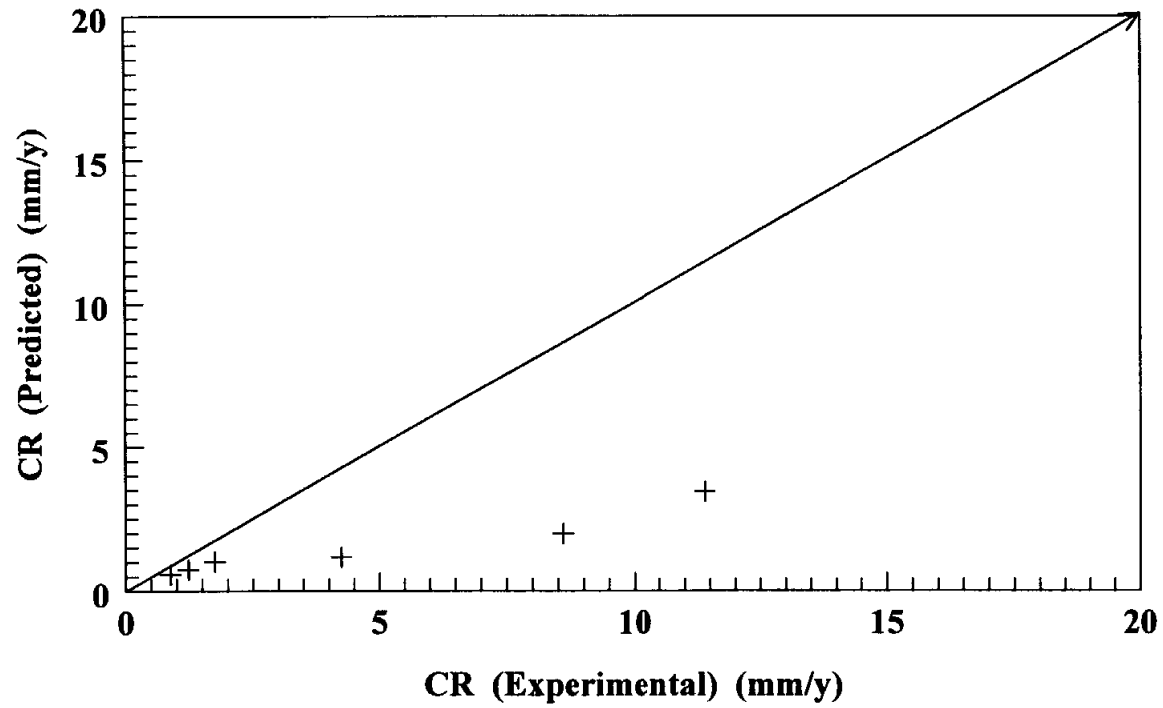


Fig 5: Predicted vs Experimental Corrosion Rates by Using Deissler Expression for Mass Transfer

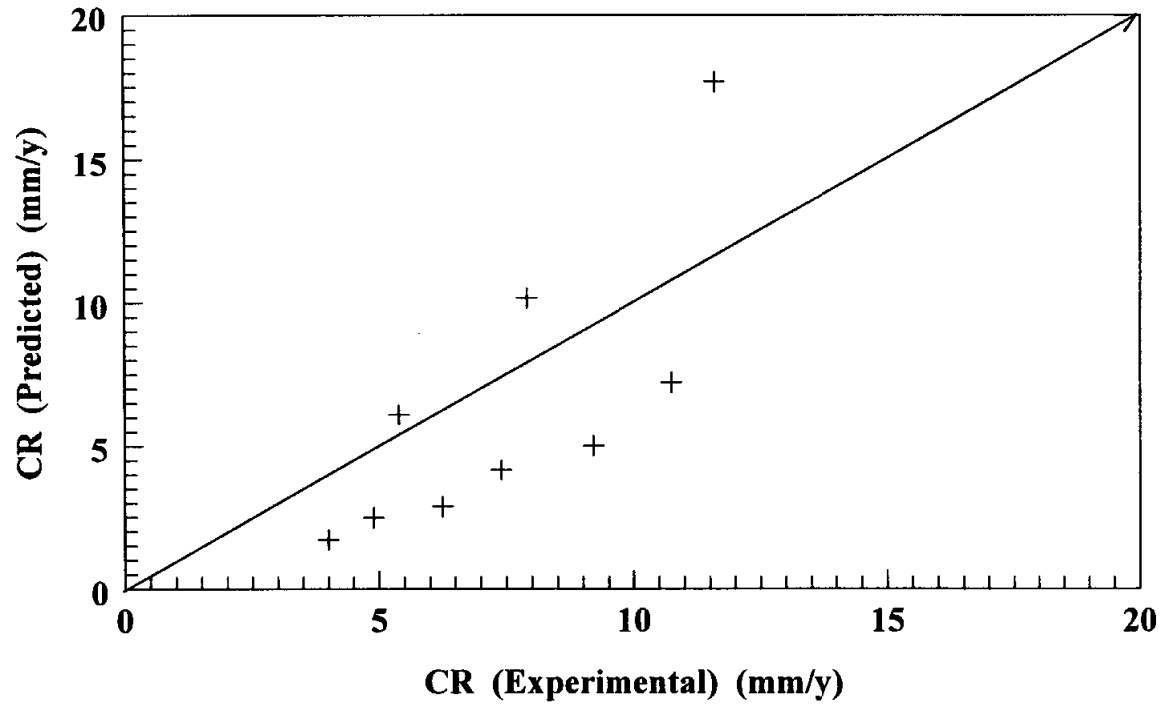


Fig 6: Predicted vs Experimental Corrosion Rates by Table 5

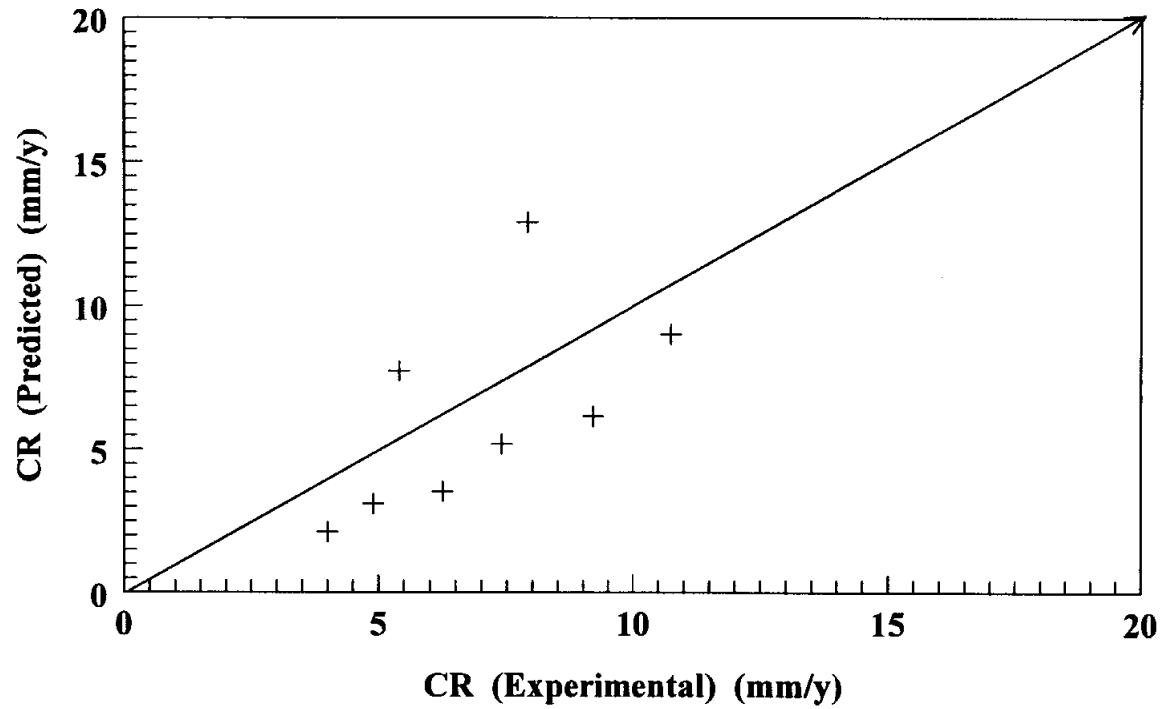


Fig8.7 Predicted vs Experimental Corrosion Rates by Table 6

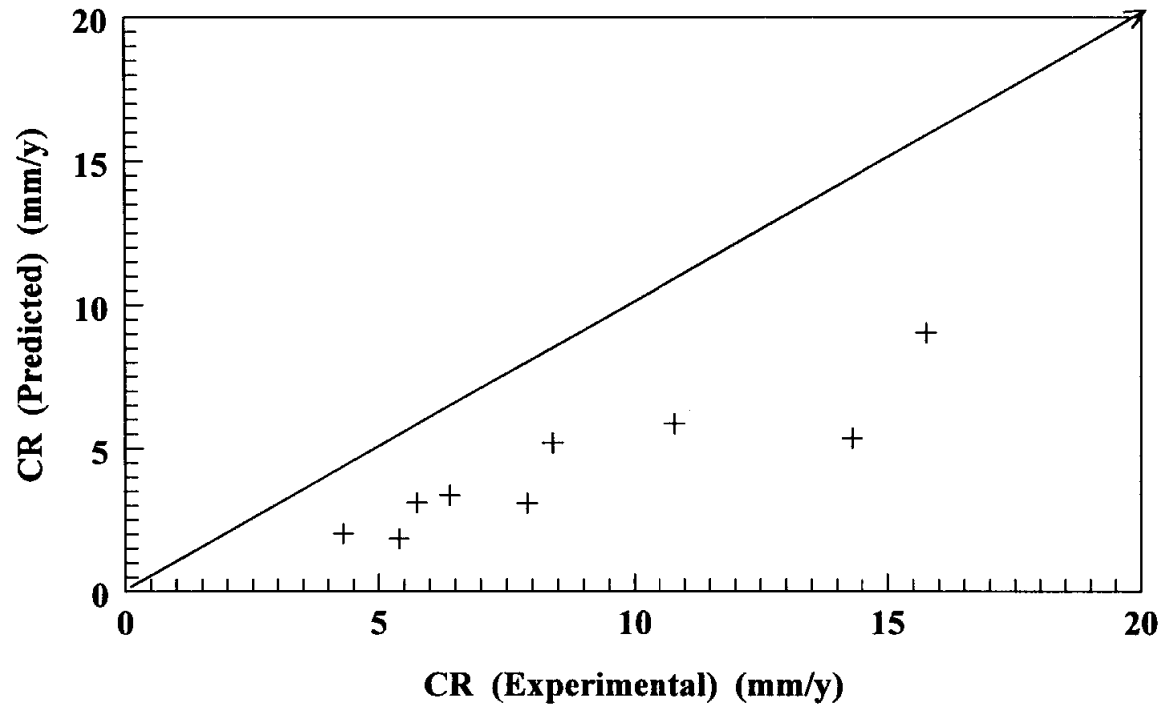


Fig 8 : Predicted vs Experimental Corrosion Rates by Table 7

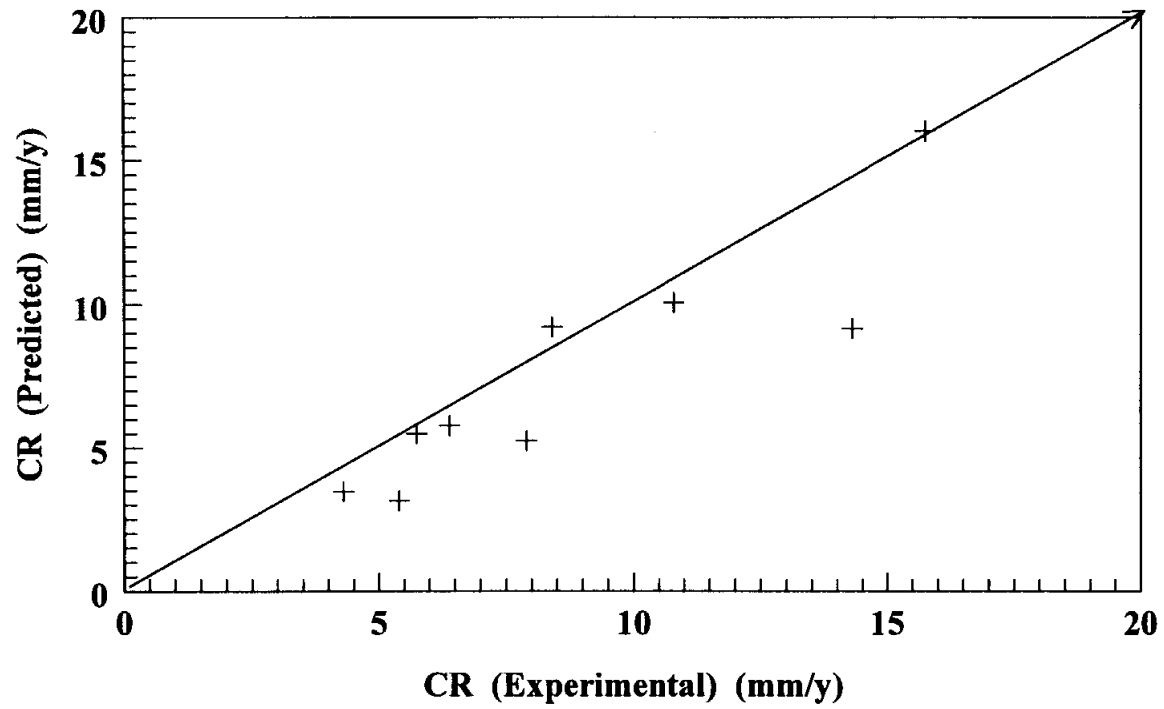


Fig 9 : Predicted vs Experimental Corrosion Rates by Table 8